Computing pseudo-crosswell data by using seismic interferometry with sources on the surface.

Adriana Gordon, Raul Cova and Kris Innanen

ABSTRACT

Seismic interferometry is a method based on the use of cross correlation and stacking operations to redatum seismic data. The special case of vertical seismic profiles (VSP) in a crosswell configuration is the interest of this study. We present an approach using seismic interferometry to compute pseudo-crosswell information. This study shows an analysis of the aperture effect and fold distribution for direct waves and full wavefield interferometry at four different maximum offsets. Results indicate that as the maximum offset increases the match between raytraced travel times and the interferometric receiver gathers improves. Using direct arrivals we were able to retrieve travel times at receivers in a lower position on the second well. However, using reflected arrivals provided travel times for receivers at shallower depths in the second well. Thus, using the full wavefield shows a more complete result. The interferometric fold distribution showed a similar result; as the maximum offset increases the fold is improved and reaches deeper parts of the model. This type of processing may help to generate data suitable for exploiting the benefits of the crosswell experiment without the risks involved in the acquisition.

INTRODUCTION

Seismic interferometry is a useful tool for computing pseudo-seismic data by cross correlation of traces recorded at different receiver locations. The key idea behind it is that the cross correlation and summation of seismic traces produces virtual events with shorter raypaths and sources located closer to the target zone (Schuster, 2009).

Wapenaar et al (2002) provided a solid mathematical foundation that give rise to the reciprocity equation of the correlation type (equation 1),

$$Im\,[D(x_B|x_A,\omega)] \approx \int D(x\,|x_A,\omega)\,D(x\,|x_B,\omega)^*\,dx, \qquad (1)$$

Where; $D(x\,|x_A,\omega)$ is the Fourier transform of the data recorded at receiver location x_A from a source located in x, and $D(x\,|x_B,\omega)^*$ is the complex conjugate of the Fourier transform of the data recorded at location x_B. This multiplication by a complex conjugate in the Fourier domain is equivalent to cross correlation in the time domain. Integration over all source locations retrieves the imaginary part of the data we would have recorded with a source at x_B and a receiver at x_A. In this version of the reciprocity equation all terms related to amplitude effects have been dropped.

This relationship may be very useful in the processing of crosswell data. Since placing sources down into a borehole may be a very risky operation. It would be very valuable to find a way of simulating this data using sources on the surface. Minato et al., (2007), applied seismic interferometry for this purpose in order to improve the imaging between wells. The basic idea for computing pseudo-crosswell data by using seismic interferometry is illustrated in Figure 1. Basically, the cross correlation of traces with

shared raypaths, cancels out the travel times in the shared portions and returns a trace with shorter travel times.

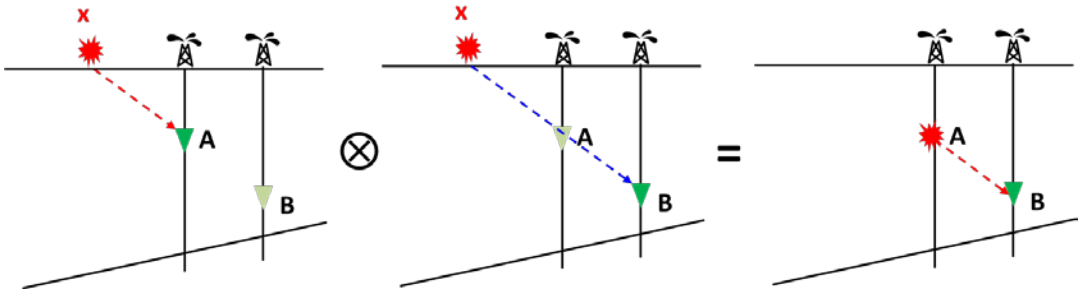

FIG. 1. Interferometric computation of pseudo crosswell seismic data using surface sources. The direct arrival to receiver A is cross correlated with the direct arrival at receiver B. The result is trace with travel times as if the source were located at A and the receiver in B.

The same principle can be used for reflected arrivals, as depicted in Figure 2. In this case the effect could be even more important because the reflector is used as a secondary source of upgoing energy. This may help to improve the range of angles covering the zone between the wells, leading to a more complete simulation of the conventional cross well experiment.

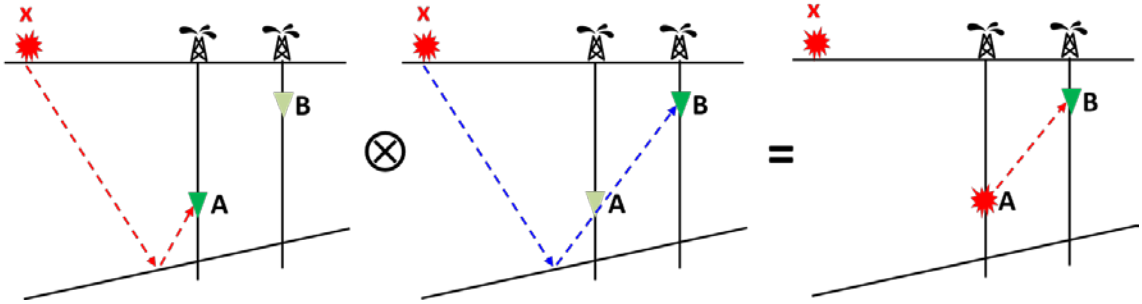

FIG. 2. Interferometric computation of pseudo crosswell data using reflected arrivals. The cross correlation of reflected arrivals that share some portion of the raypath returns traces with shorter raypath as if the source were down in the borehole.

In addition to the relief of not having sources down in the borehole, this method may allow us to record data with better energy even at large well separations. Due to the risk of causing damage to the borehole, crosswell seismic sources tend to be very weak in power. This poses a limitation in the maximum separation between wells. However, if sources are located on the surface we should be able to use sources with enough seismic energy to cover large distances between wells.

In the following sections, experiments using synthetic data will be shown. The effect of the source-to-well offset on the pseudo-receiver gather generation will be addressed. We will also dedicate a section to study how the coverage of the area between wells evolves.

DIRECT ARRIVALS INTERFEROMETRY

Aperture effect

In order to perform an analysis of seismic interferometry in a crosswell configuration, it is important to understand the process. The first step is to cross correlate a receiver gather from one well with another receiver gather in the second well and then stack the result. The outcome will be a single trace as show in Figure 3. The peak of the cross correlation function in this case matches the travel time between the two receivers.

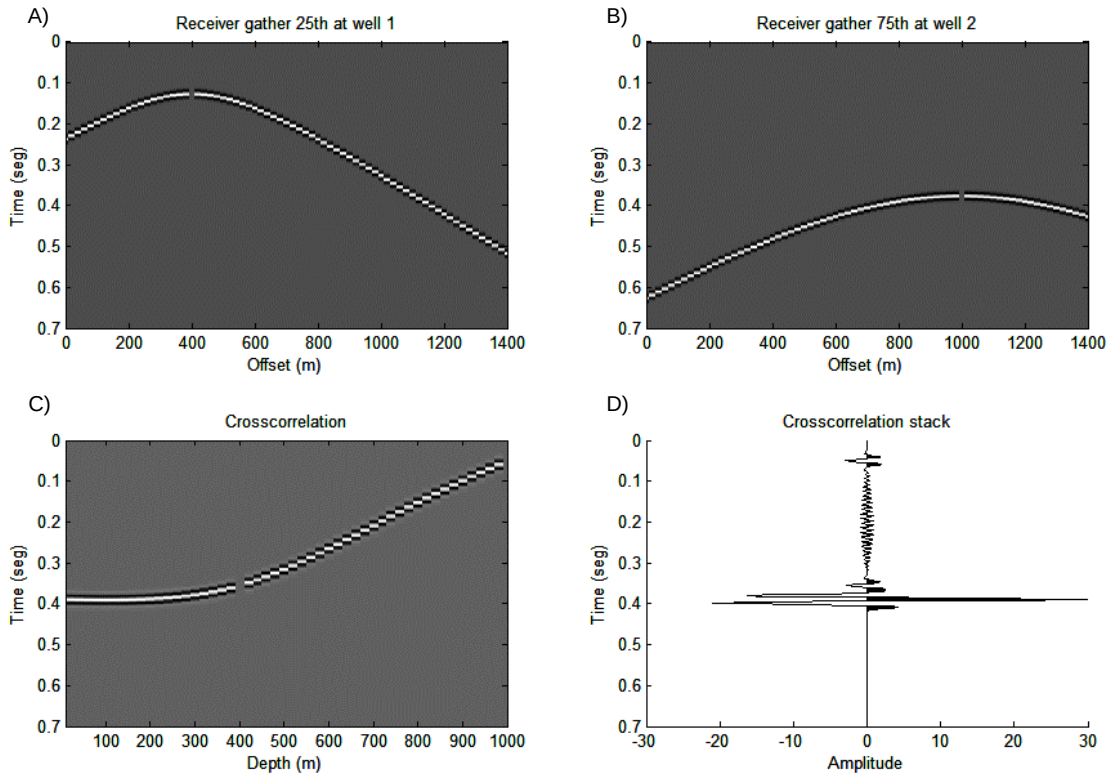

Fig. 3. Interferometric computation of a pseudo-crosswell trace. Two receiver gathers (A) and (B) at different depths from each well are cross correlated (C) and stacked (D). The result is a seismic trace with a shorter travel time corresponding to the travel time between both receivers.

This method was repeated for all the receivers in both wells. The result is a set of traces as shown in Figure 4. This seismic gather simulates a receiver gather recorded at well 2 as if the source had been placed in well 1.

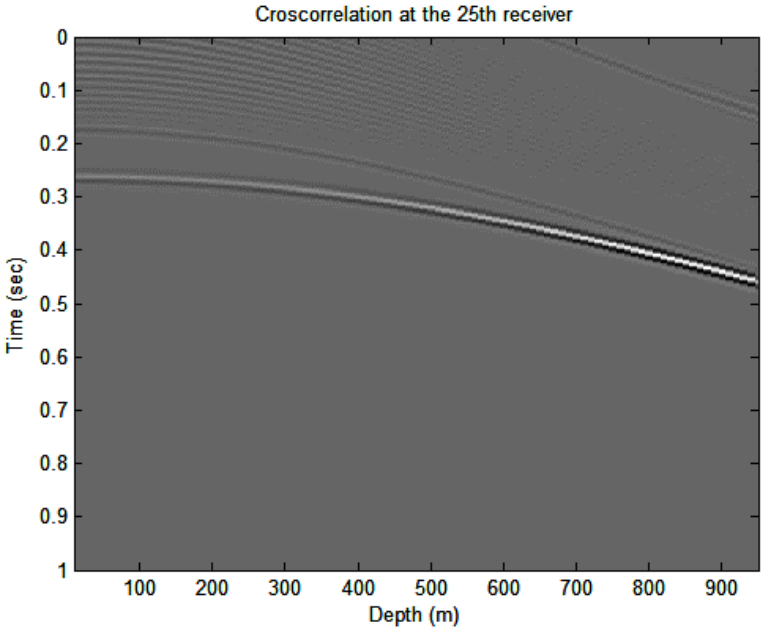

Fig. 4. Pseudo-crosswell receiver gather.

Once the seismic interferometry procedure was completed for all the receivers in both wells, the result was plotted with the superposition of the raytraced travel times, in order to verify the quality of the outcome. This process was repeated for four different maximum offsets, 1000m, 2000m, 3000m and 4000m. Figures 5 to 8 display the results at three different depths corresponding to the 50m, 500m and 750m receiver depth for each maximum offset.

Since in this part we deal with downgoing waves, only the pseudo-traces computed at receivers with larger depths than the reference depth in well 1 are considered reliable. This limit is illustrated with a red line according to each case. Amplitude trace equalization was applied to all the cross correlations due to the presence of spurious events with high energy which may overshadow the events of interest.

For the 1000m offset (Figure 5) we can see for the shallowest receiver location, that the timing of the events in the pseudo-receiver gather matches the travel times computed by raytracing. However, as the receiver depth increases the match is lost for all the traces.

After increasing the offset to 2000m (Figure 6), there is an important improvement for the middle receiver. On the other hand, the deep receiver gather starts to show some agreement with the raytraced travel times.

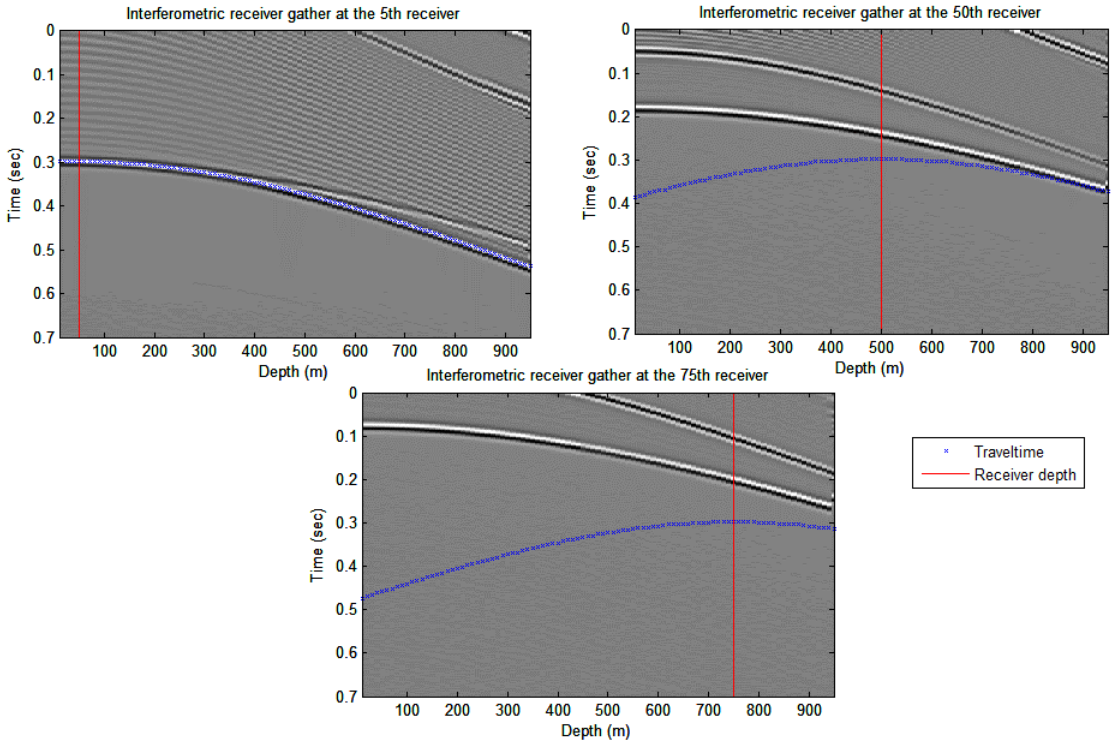

Fig. 5. Pseudo receiver gathers at depths of 50m, 500m and 750m for an offset of 1000m.

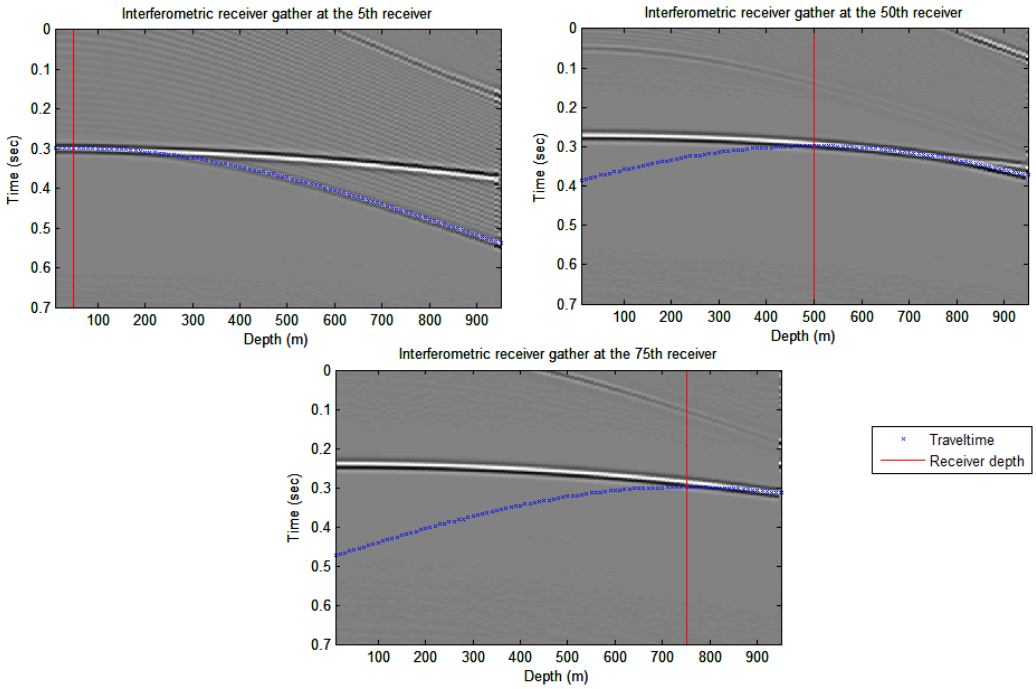

Fig. 6. Pseudo receiver gathers at depths of 50m, 500m and 750m for an offset of 2000m.

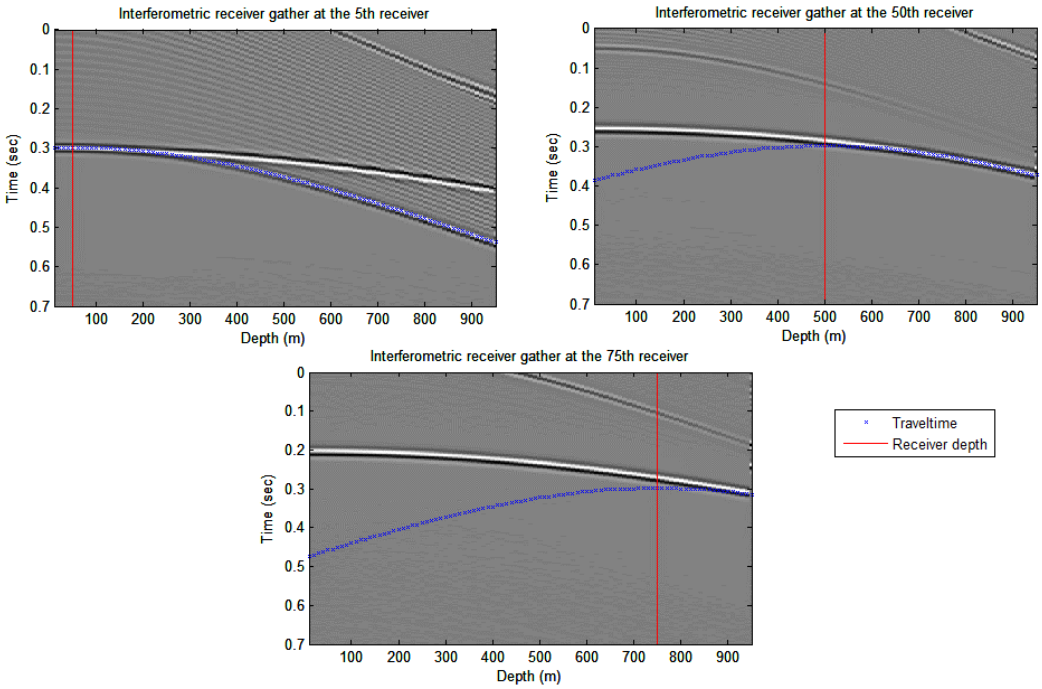

Fig. 7. Pseudo receiver gathers at depths of 50m, 500m and 750m for an offset of 3000m.

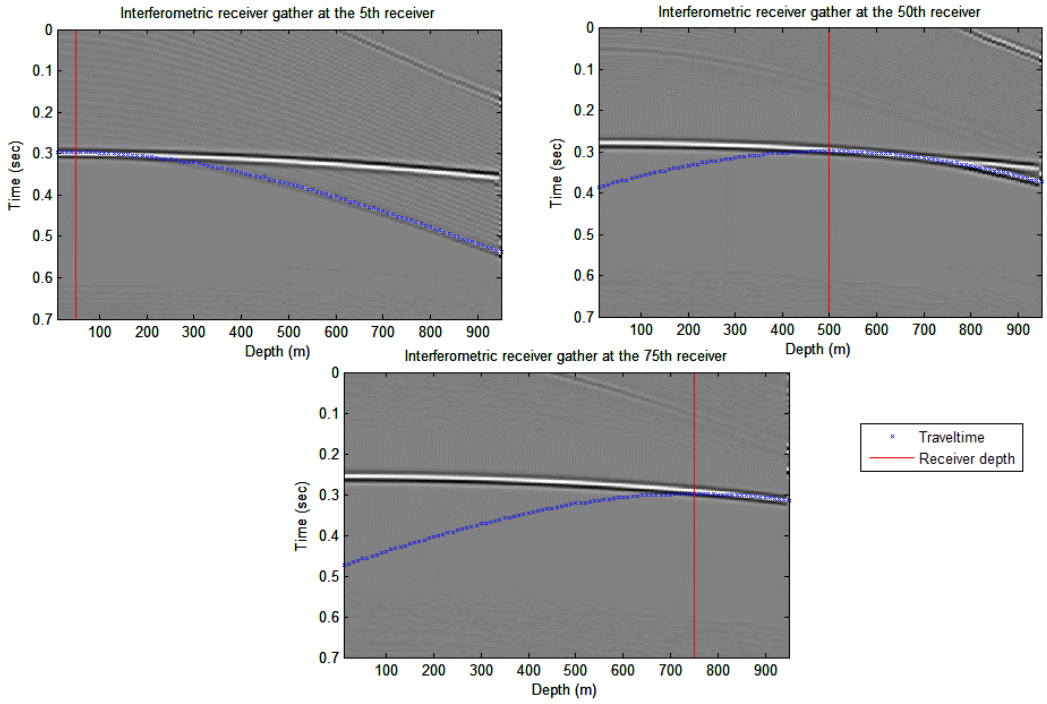

Fig. 8. Pseudo receiver gathers at depths of 50m, 500m and 750m for an offset of 4000m.

In Figure 7 we can see how, at a 3000m offset, the reconstructed events show a very good match to the raytraced travel times for all the depths.

For a maximum offset of 4000m (Figure 8), an excellent match between the cross correlation and the raytraced travel time is achieved for all the receivers.

In summary, for small maximum offsets cross-correlation at the deeper receivers does not match the raytraced travel times. As the maximum offset increases the relation between these two parameters improves. The reason for this is that at larger offsets the wavefield arrives with wider angles at both wells. Then, a larger range of receivers are excited for the same wavefield. When offsets are short, raypaths are almost vertical, as a result only deeper receivers in the second well record useful information for the interferometric processing.

Fold distribution

In this section we show fold maps for each case of maximum offset. Figures 9 to 12 display both wells with the receivers in red and the reflector at 950 meters in white. The color bar at the right indicates the number of times a ray traveled through that part of the model.

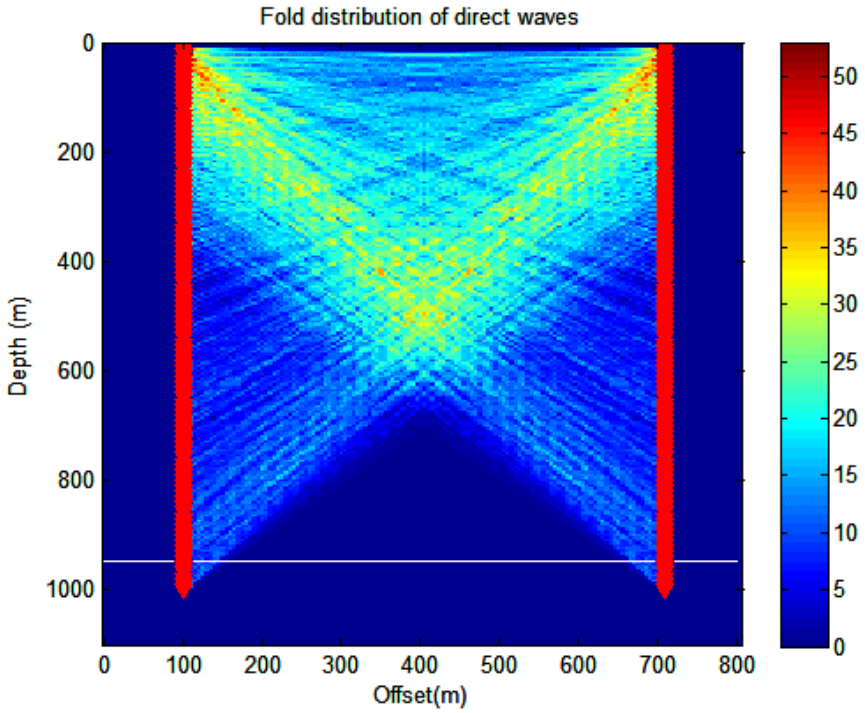

Fig. 9. Fold map for a maximum offset of 1000 m.

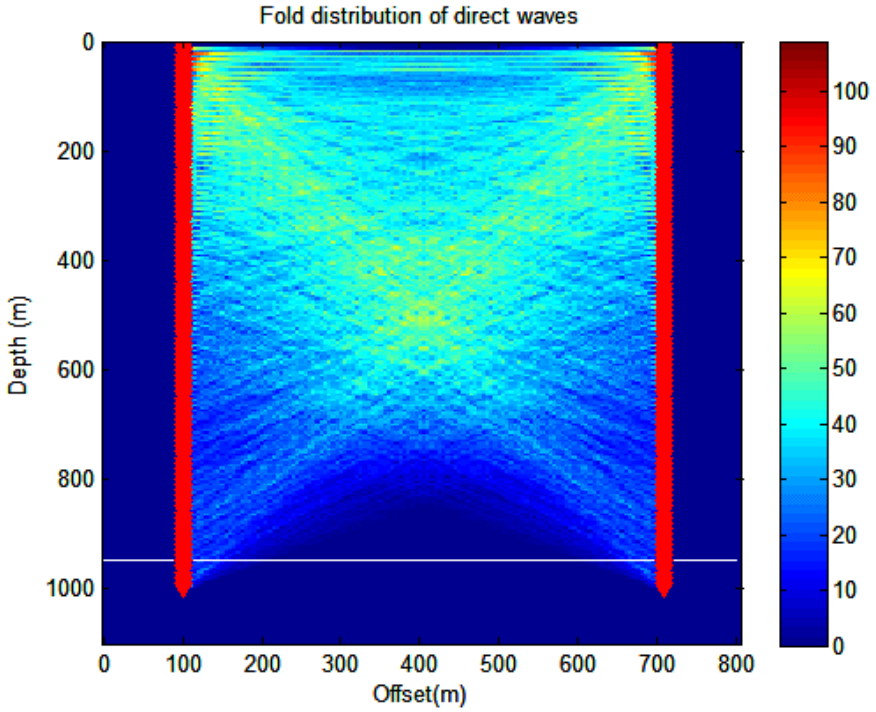

Fig. 10. Fold map for a maximum offset of 2000 m.

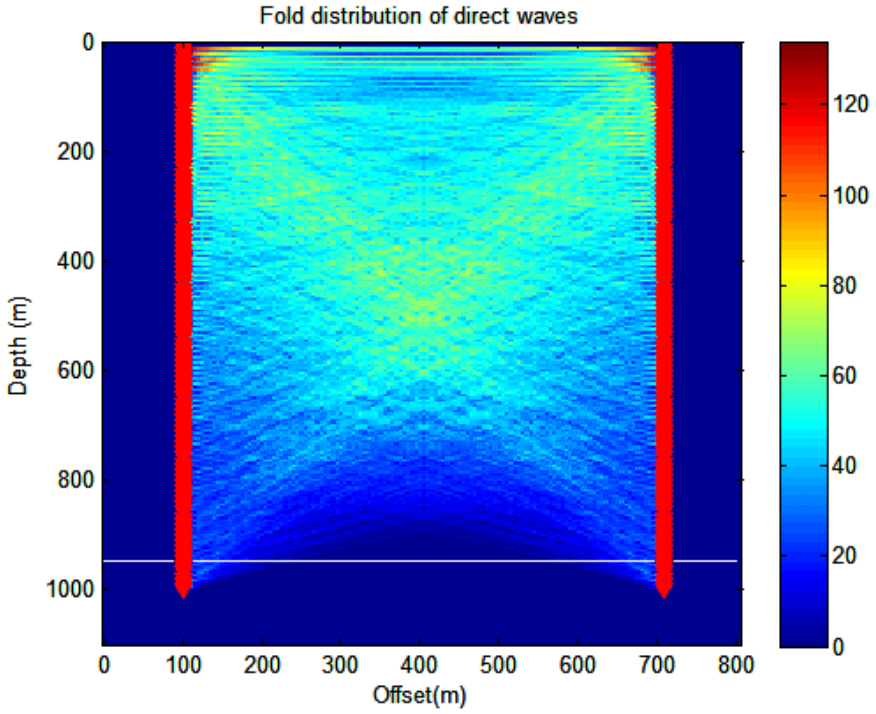

Fig. 11. Fold map for a maximum offset of 3000 m.

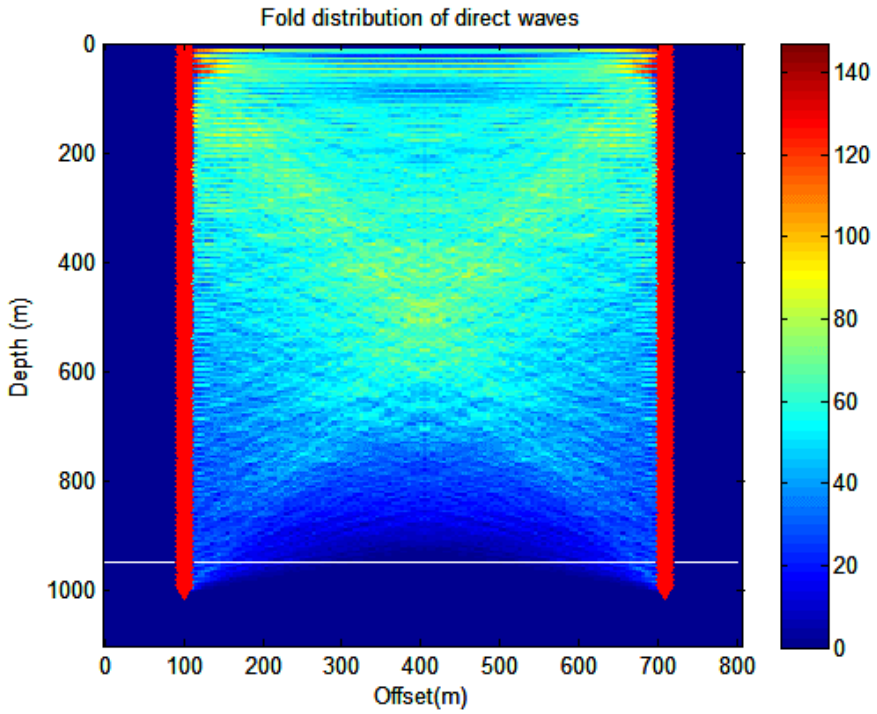

Fig. 12. Fold map for a maximum offset of 4000 m.

As we can see in Figure 9, maximum offsets of small length, e.g. 1000m do not yield a significant fold in the deeper part of the model. As the maximum offset increases the fold in the deepest part of the model improves. For a maximum offset of 4000meters (Figure 10) there is a fold that almost completely reaches the depth of the reflector.

Full wavefield interferometry

Aperture effect

In the case of full wavefield interferometry, we used the same procedure as for direct arrivals. Figures 13 to16 show the pseudo-receiver gathers with the raytraced travel times overlaid on the plots for the four different offset used. Since downgoing and upgoing waves are now included, we expect to obtain useful data from a wider extent of the well. The red line displayed in the images indicates the depth location of the receiver which will be useful later to compare the direct and full wavefield results. A gain function was also applied in this case to equalize the amplitudes along the traces.

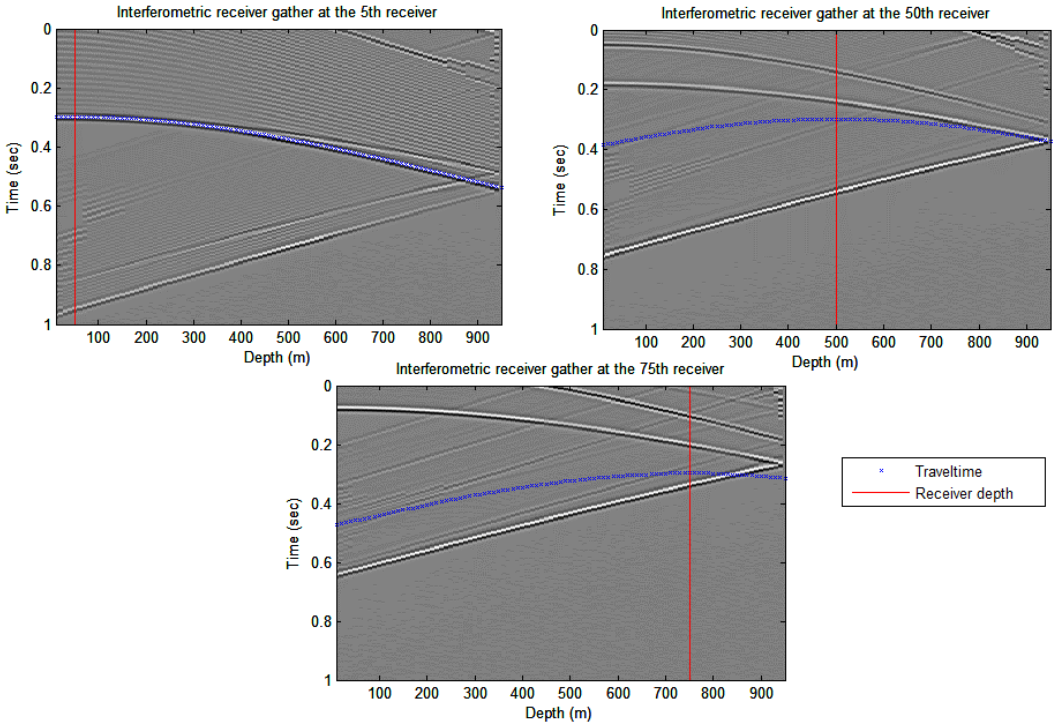

Fig. 13. Pseudo-receiver gathers at depths of 50m, 500m and 750m for an offset of 1000m. Both direct arrivals and reflected arrivals are used in the interferometric processing.

In Figure 13 it is possible to notice that the pseudo-traces match only the raytraced travel time for the shallowest receiver gather at 50 meters depth. For the other two receiver gathers the correlation is poor. The receiver gather at 500m shows a limited agreement at the greater depths. In the case of the receiver at 750m, there is no agreement between the pseudo-traces and the raytraced travel times of the first arrivals.

For a maximum offset of 2000m (Figure 14) good improvement is shown for the receiver at 500m. The deepest receiver now starts to show some agreement for shallow and deep traces. However, between 500m and 800m the stacked cross correlations show very poor energy.

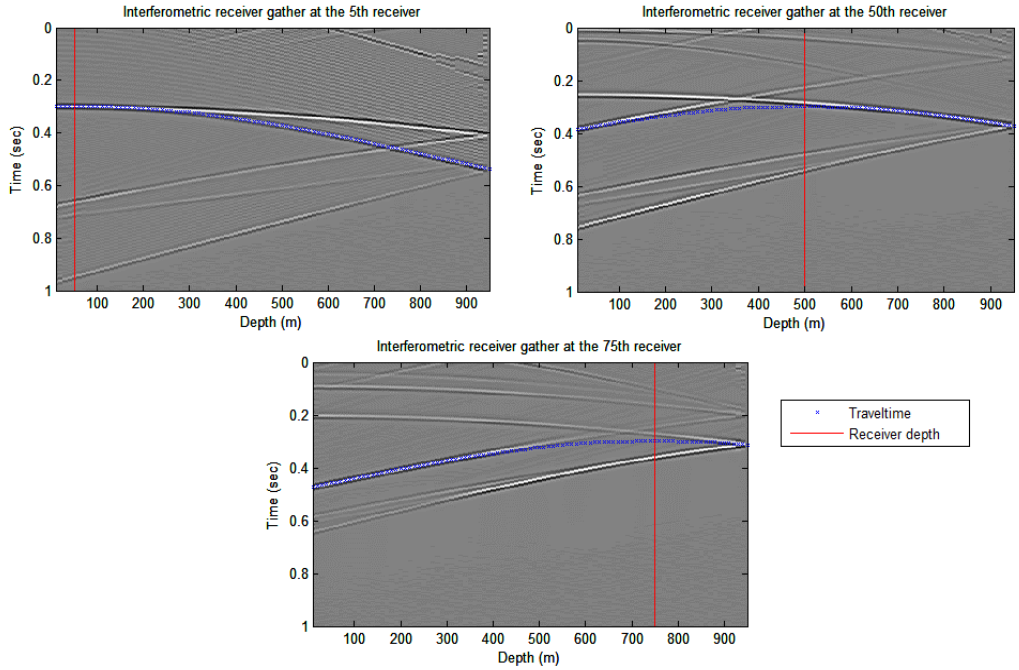

Fig. 14. Pseudo-receiver gathers at depths of 50m, 500m and 750m for an offset of 2000m. Both direct arrivals and reflected arrivals are used in the interferometric processing.

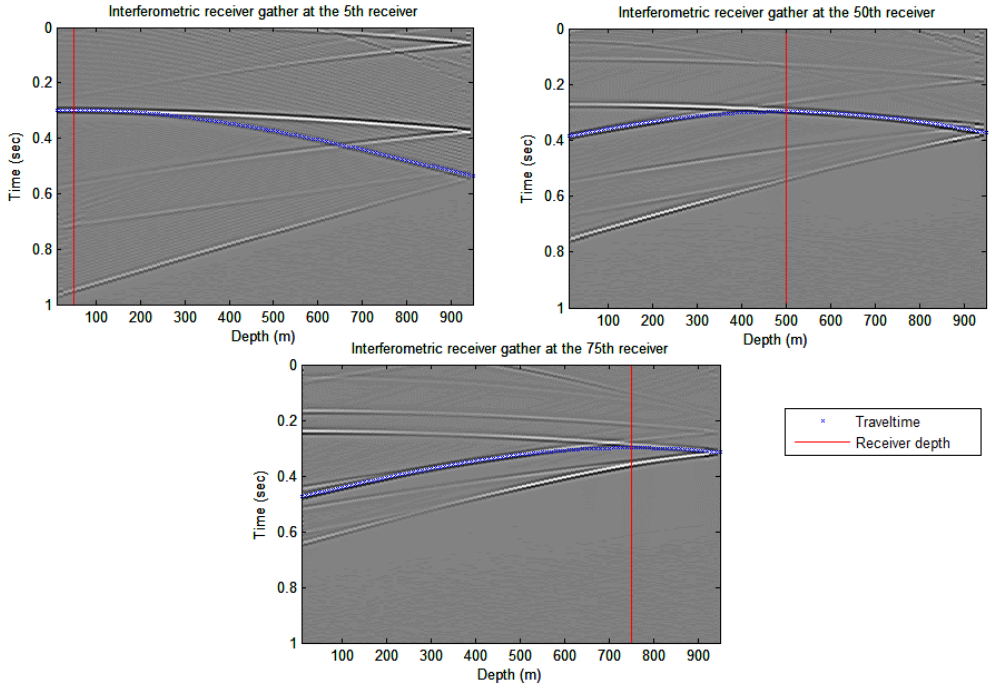

Fig. 15. Pseudo-receiver gathers at depths of 50m, 500m and 750m for an offset of 3000m. Both direct arrivals and reflected arrivals are used in the interferometric processing.

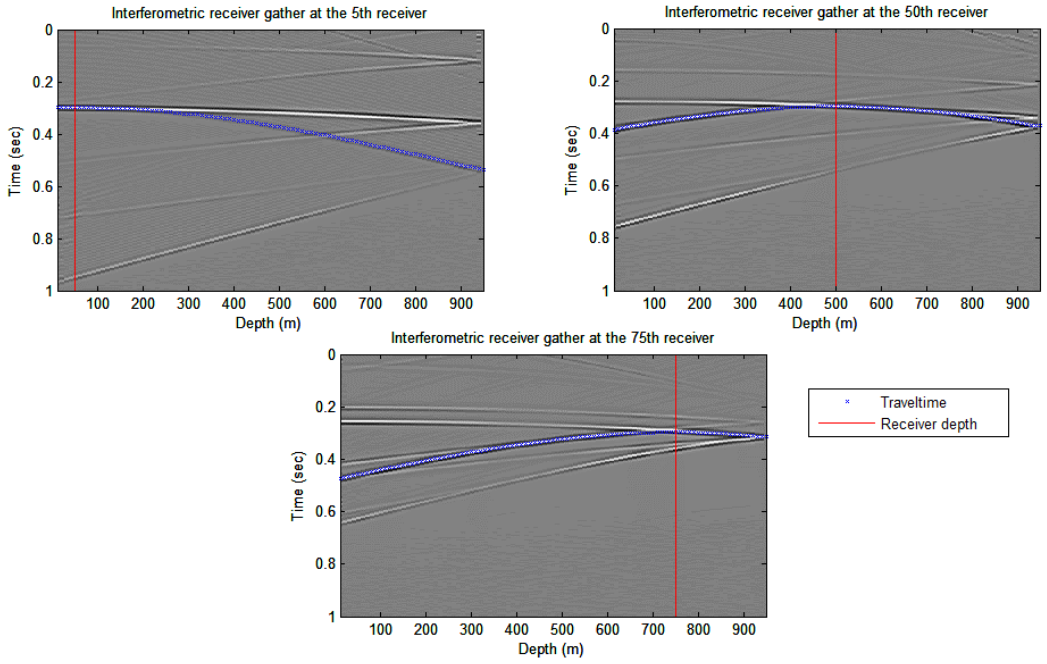

Fig. 16. Pseudo-receiver gathers at depths of 50m, 500m and 750m for an offset of 4000 m. Both direct arrivals and reflected arrivals are used in the interferometric processing.

With a maximum offset of 3000m (Figure 15), it is possible to notice improvements for the deeper receivers. Both the 500m and 750m receivers present a very good match between the pseudo-traces and the raytraced travel time of the direct arrivals.

Increasingly, the offset to 4000m (Figure 16) does not provide an important improvement in the traces. It seems for this configuration, a maximum offset of 3000m is enough for retrieving pseudo-crosswell data that matches the raytraced travel times.

In summary, as the maximum offset increases the relationship between the pseudo-traces and the raytraced travel times get better for the deeper receivers. Another important observation is that reflected upgoing waves are easily identified in the four cases. They all have a completely different moveout. They can also be identified by examining the depth where the downgoing and the upgoing waves converge, which should be at the reflector's depth (950m).

Fold distribution

Figures 17 to 20 show the fold maps obtained when using the full wavefield (reflections and direct arrivals) for each maximum offset. As in the case of direct arrivals, the images display two wells with red receivers, and a reflector at 950 meters in white. The color bar at the right denotes the number of times a ray traveled through that part of the model.

Figure 17 does not show fold for the reflected waves: this may be a result of using a short maximum offset. At this offset no upgoing legs in the reflection raypath intersect both wells.

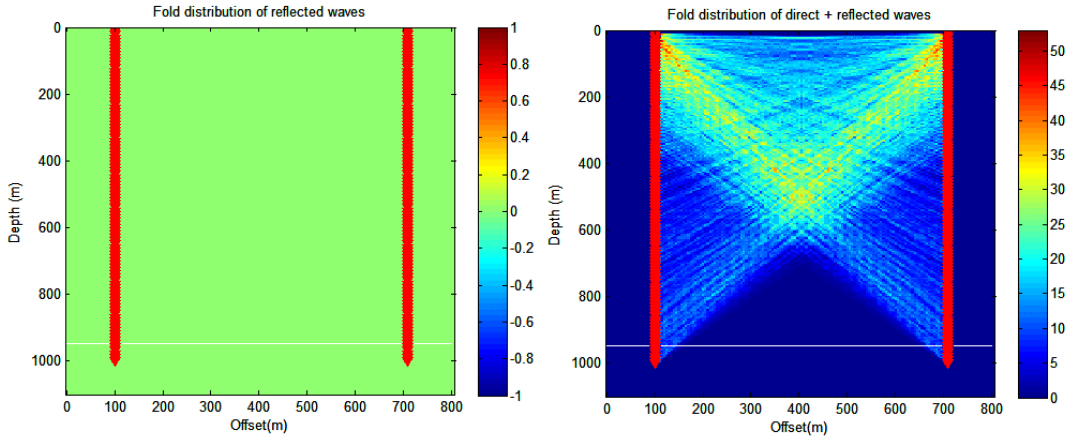

Figure 17 Fold map for a maximum offset of 1000 m.

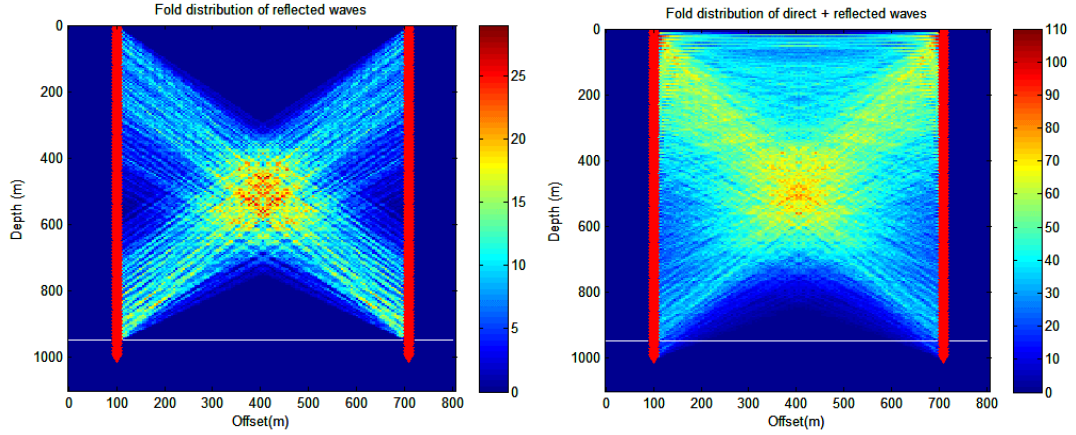

Figure 18 Fold map for a maximum offset of 2000 m.

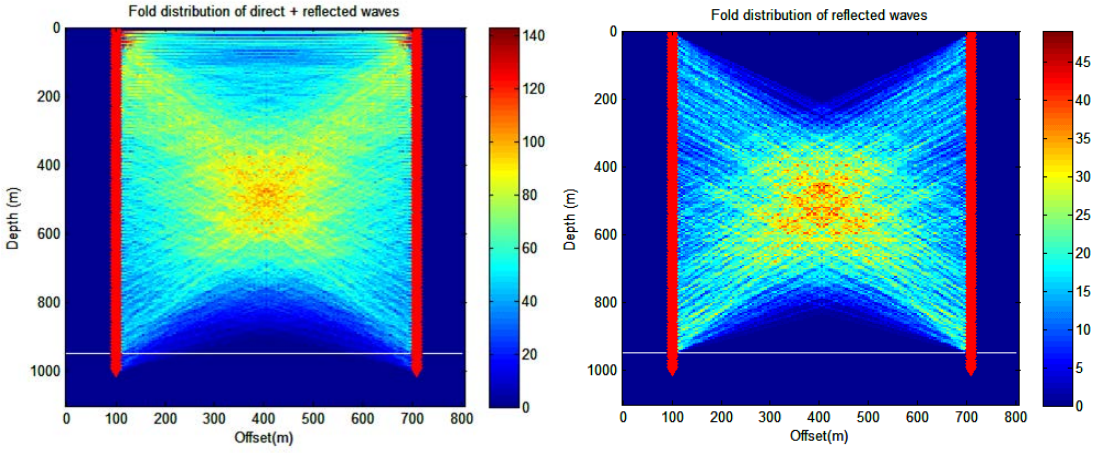

Figure 19 Fold map for a maximum offset of 3000 m.

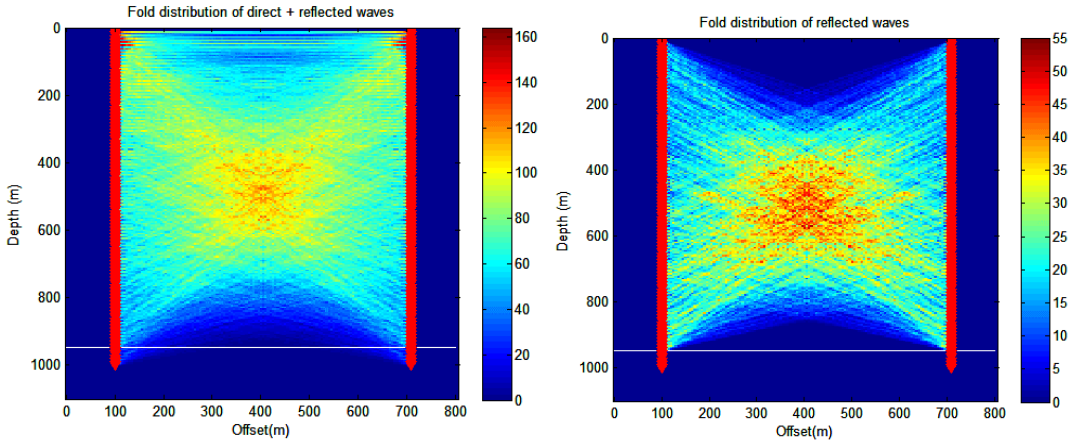

Figure 20 Fold map for a maximum offset of 4000 m.

In general, the previous images show that small maximum offsets do not present fold in the deepest part of the model. As the maximum offset increases, the fold in the deepest part of the model also improve for both the reflected and the direct plus reflected waves cases.

To understand the difference between the results of direct arrival interferometry and full wavefield interferometry, Figure 21 presents both cases for an offset maximum of 4000 meters. On the left is the direct arrival interferometric receiver gather for the receiver at 750m depth, and on the right the full wavefield interferometric receiver gather for the same receiver. At first look it may be noticed that the image on the right has more events than the left one.

At the left of the red lines in Figure 21 some differences are evident.

In the direct arrival image no signal matches the travel time from the left side of the red line. Therefore, as explained in the first part of the results, this side was not considered reliable. On the other hand, at the left side of the red line for the full wavefield image, there is indeed a matching signal all across the survey. Thus, the upgoing waves provided the signal needed to retrieve reliable pseudo-traces at those depths.

Another important analysis is the comparison between a conventional crosswell fold and an interferometric fold. In Figure 22 we show the fold maps for the 4000m offset case and the one given by a conventional crosswell acquisition.

The conventional crosswell fold map was created locating the sources at the position of the receivers, i.e. there were shooting rays from each side of the wells. Hence, the map has a symmetric appearance. Comparing these results with the highest fold obtained with the interferometric crosswell fold maps, the first item we note is the difference in the maximum fold in the model. The conventional crosswell fold exceeds by far the maximum fold of the best interferometric fold outcome.

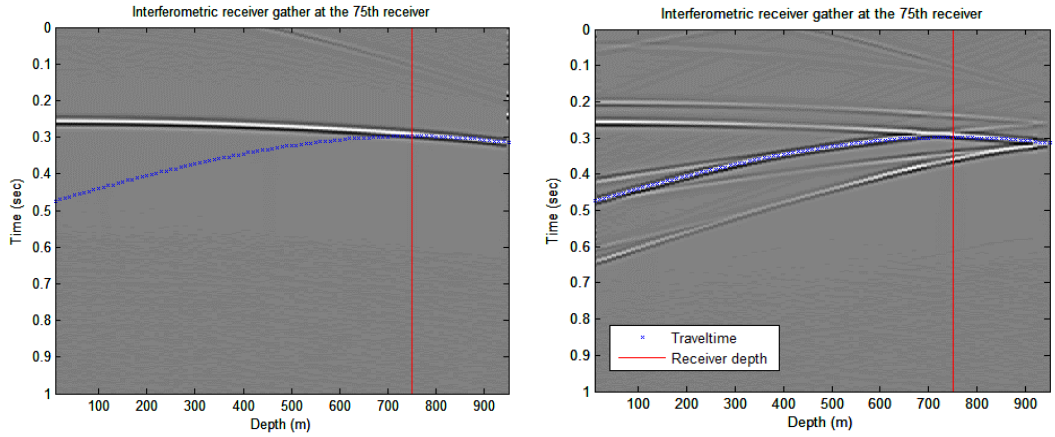

Fig. 21. Interferometric receiver gather comparison for a maximum offset of 4000m. (left) Using only direct arrivals. (right)

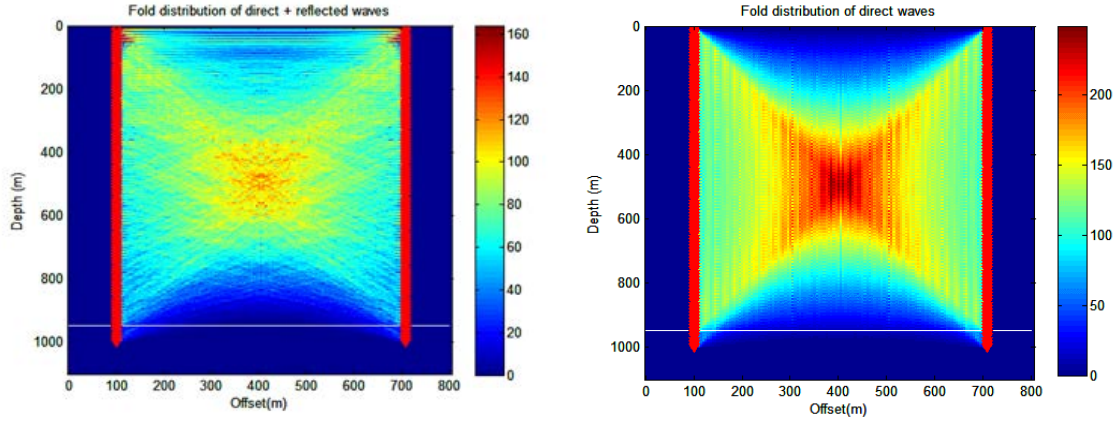

Fig. 22. Fold comparison. (left) of Interferometric fold map for a full wavefield at a maximum offset of 4000m Conventional crosswell fold map (right) for direct arrivals.

However, the interferometric result displays a well distributed fold along the model. This is an important requirement for seismic tomography studies. Both Figures achieve illumination of almost all the model effectively, and, in a similar way, they reach the deepest part of it.

CONCLUSIONS

Seismic interferometry is a method of cross-correlating traces recorded at different locations to retrieve subsurface information. This paper has shown an approach where the use of seismic interferometry can be helpful to reconstruct crosswell information that was not available with the conventional methods. The analysis of the aperture effect showed that as the maximum offset increases, the relation between the timing of the pseudo-traces and the raytraced travel times improves. We also noted that this agreement is more complete when the full wavefield is used in the in the processing. The fold distribution has a similar result, by increasing the maximum offset we were able to reach the deepest part of the model. Although the conventional crosswell fold yields superior results than

the interferometric crosswell fold, the latter one may be good enough for performing a tomographic inversion.

FUTURE WORK

These achievements provide an opportunity to attempt towards further use of seismic tomography for computing a velocity model between the two wells. Also, we think the use of converted waves events will be of important interest. Including these procedures, we may be able to compute both P- and S-wave velocity models using tomographic methods.

ACKNOWLEDGEMENTS

We thank CREWES and its sponsors for the opportunity to develop this research. We also gratefully acknowledge support from NSERC (Natural Science and Engineering Research Council of Canada) through the grant CRDPJ 379744-08. Our further thanks to Raul Cova for his guidance during this research and Kris Innanen for his support.

REFERENCES

Minato, S., K. Onishi, T. Matsuoka, Y. Okajima, J. Tsuchiyama, D. Nobuoka, H. Azuma, and T. Iwamoto, 2007, Crosswell seismic survey without borehole source: 77th Annual International Meeting, SEG, Expanded Abstracts, 1357–1361.

Schuster, G., 2009, Seismic Interferometry: Cambridge University Press.

Wapenaar, K., 2004, Retrieving the elastodynamic Green's function of an arbitrary inhomogeneous medium by cross correlation: Physical Review Letters, 93, 254,301.1–254,301.4.